A&A 468, L29–L32 (2007)
DOI: 10.1051/0004-6361:20077387


Astronomy & Astrophysics
Special feature

*Extended baselines for the IRAM Plateau de Bure interferometer: First results*

Letter to the Editor

# PdBI sub-arcsecond study of the SiO microjet in HH212

## Origin and collimation of class 0 jets

S. Cabrit[1], C. Codella[2], F. Gueth[3], B. Nisini[4], A. Gusdorf[5], C. Dougados[6], and F. Bacciotti[7]

[1] LERMA, UMR 8112 du CNRS, Observatoire de Paris, 61 Av. de l'Observatoire, 75014 Paris, France
e-mail: sylvie.cabrit@obspm.fr
[2] INAF, Istituto di Radioastronomia, Sezione di Firenze, Largo E. Fermi 5, 50125 Firenze, Italy
[3] IRAM, 300 rue de la Piscine, 38406 Grenoble Cedex, France
[4] INAF-Osservatorio Astrofisico di Roma, via di Frascati 33, 00040 Monte Catone, Italy
[5] Physics Department, The University, Durham DH1 3LE, UK
[6] Laboratoire d'Astrophysique de l'Observatoire de Grenoble, BP 53, 38041 Grenoble Cedex, France
[7] INAF-Osservatorio Astrofisico di Arcetri, Largo E. Fermi 5, 50125 Firenze, Italy

Received 1 March 2007 / Accepted 3 April 2007

**ABSTRACT**

*Context.* The bipolar HH 212 outflow has been mapped in SiO using the extended configuration of the Plateau de Bure Interferometer (PdBI), revealing a highly collimated SiO jet closely associated with the $H_2$ jet component.
*Aims.* We study at unprecedented resolution (0.″34 across the jet axis) the properties of the innermost SiO "microjet" within 1000 AU of this young Class 0 source, to compare it with atomic microjets from more evolved sources and to constrain its origin.
*Methods.* The SiO channel maps are used to investigate the microjet collimation and velocity structure. A large velocity gradient analysis is applied to SiO (2−1), (5−4) and (8−7) data from the PdBI and the Submillimeter Array to constrain the SiO opacity and abundance.
*Results.* The HH212 Class 0 microjet shows striking similarities in collimation and energetic budget with atomic microjets from T Tauri sources. Furthermore, the SiO lines appear optically thick, unlike what is generally assumed. We infer $T_k \simeq 50-500$ K and an SiO/$H_2$ abundance $\geq 4\times10^{-8}-6\times10^{-5}$ for $n(H_2) = 10^7-10^5$ cm$^{-3}$, i.e. 0.05−90% of the elemental silicon.
*Conclusions.* This similar jet width, regardless of the presence of a dense envelope, definitely rules out jet collimation by external pressure, and favors a common MHD self-collimation (and possibly acceleration) process at all stages of star formation. We propose that the more abundant SiO in Class 0 jets could mainly result from rapid (≤25 yrs) molecular synthesis at high jet densities.

**Key words.** stars: formation – radio lines: ISM – ISM: jets and outflows – ISM: molecules – ISM: individual objects: HH212

## 1. Introduction

Millimeter interferometric studies of the L1448 and HH211 Class 0 sources have identified high-velocity SiO jet-like emission possibly related to the primary protostellar wind (Guilloteau et al. 1992; Chandler & Richer 2001; Hirano et al. 2006; Palau et al. 2006; Gueth et al. 2007). A similar SiO jet has recently been discovered by Codella et al. (2007, hereafter Paper I) in the HH212 $H_2$ outflow in Orion ($d \simeq 450$ pc) using the new extended configuration of the PdBI. This study revealed highly collimated SiO emission with a close spatial and kinematic correspondence to near-IR $H_2$ knots, indicating that both are tracing the same molecular jet component. In addition, an inner pair of SiO knots with no near-IR $H_2$ counterparts was identified at ±1.″5 of the central source, with a radial velocity range pointing to a high degree of collimation. Continuum data at 1mm further reveal a compact, optically thick source probably tracing a disk of diameter ≤ 120 AU. Similar conclusions were reached by Lee et al. (2007) in a lower resolution, multi-species study with the Submillimeter Array (SMA).

In this second paper, we further exploit the unprecedented resolution of 0.″34 *HPBW* across the jet axis provided by the extended configuration of the PdBI to carry out the first comparison of the properties of the Class 0 SiO "microjet" in HH212 with atomic microjets from Class I/II sources observed on similar scales. We identify several similarities suggesting that the same collimation (and possibly acceleration) mechanism is at work in Class 0 jets as in later stages. We also demonstrate that SiO is optically thick and close to LTE in the inner knots (as is not generally assumed) and discuss possible origins for the abundant SiO in Class 0 jets, compared to their more evolved counterparts.

## 2. Jet collimation and velocity structure

### 2.1. Present SiO observations

Figure 1 presents PdBI SiO 5–4 maps from Paper I of the inner jet knots, separated into three velocity intervals. The SiO microjet is *extremely narrow*, with a typical transverse *FWHM* ≃ 0.″4 at all velocities, i.e. an intrinsic width of 0.″2 = 90 AU after correction for the PdBI *HPBW* of 0.″34 in the same direction[1].

[1] A slightly larger width of 0.″35 was quoted in Paper I, where cleaning had not been optimized for the innermost jet regions.

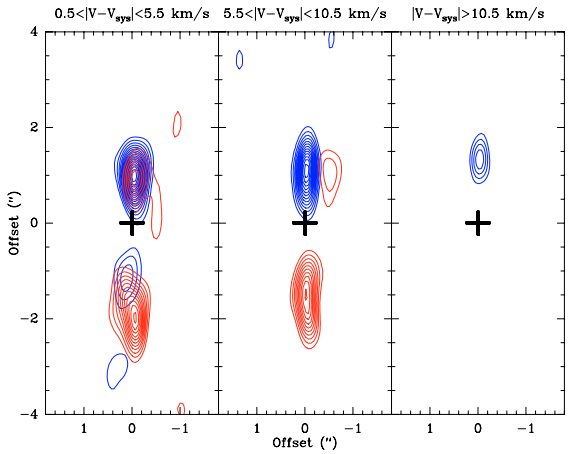


**Fig. 1.** SiO (5–4) emission maps of the HH212 microjet in 3 different velocity ranges. Blue and red contours refer to blueshifted and redshifted gas, respectively. A cross marks the position of the continuum source from Paper I: $\alpha(2000) = 05^h43^m51\overset{s}{.}41$, $\delta(2000) = -01°02'53\overset{''}{.}160$. Contour spacing is 50 mJy/beam km s$^{-1}$ with the first contour at 100 mJy/beam km s$^{-1}$.

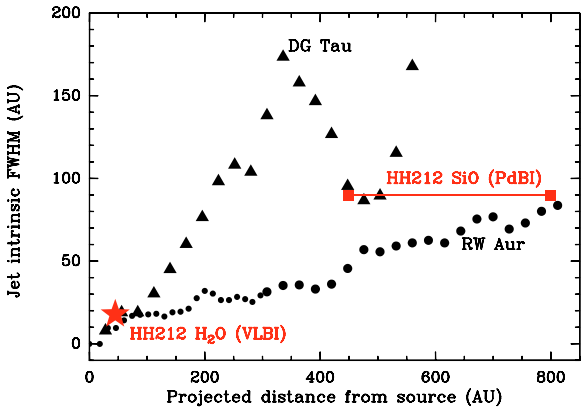


**Fig. 2.** HH212 intrinsic jet width compared to the range spanned by atomic microjets from Class II sources, corrected for the instrumental PSF (small dots: Woitas et al. 2002; large dots and triangles: Dougados et al. 2000); Our SiO PdBI measurements are shown as filled squares; the $H_2O$ maser width from Claussen et al. (1998) as a filled star.

Figure 1 also shows that, in both lobes, the region of blue/red overlap is not coincident with the region of highest radial velocities, but is slightly *trailing behind it* by about 0.″4. The lack of blue/red contamination towards the fastest gas requires that its motions are highly forward-directed with a semi-opening angle ≤4° (see Paper I). The blue/red overlap at low velocities ≃3−4 km s$^{-1}$ traces less collimated, slower material in the wake of the fastest gas.

### 2.2. Comparison with jets from more evolved sources

The width of atomic jets from T Tauri Class II sources spans a relatively broad range, depending on the brightness of bow-shock wings driven by internal working surfaces. In Fig. 2, the intrinsic *FWHM* of the HH212 SiO microjet is compared to the broadest (DG Tau) and narrowest (RW Aur) atomic microjets from Class II sources studied so far using ground-based adaptive optics or HST (Dougados et al. 2000; Woitas et al. 2002). We find that the HH212 SiO microjet falls exactly in the same range as Class II jets on scales 500−1000 AU. Similar results are found for the SiO jet from the HH211 Class 0 source (width of 95−125 AU at distances of 300−600 AU; Gueth et al. 2007).

Also indicated in Fig. 2 is the width of the HH212 jet at 50 AU from the source, ≃40 mas = 18 AU, as inferred from the bow shape of $H_2O$ maser spots within 100 mas (Claussen et al. 1998). Again it is undistinguishable from that of atomic microjets at the same distance. We thus find no evidence of a higher jet collimation in Class 0 sources compared to the T Tauri stage where only a thin disk is present, although the dense infalling envelopes characterizing the Class 0 stage would be capable of strongly reconfining a radially expanding wind (Delamarter et al. 2000). This definitely rules out collimation by external pressure gradients and requires that jets from young stellar objects are self-collimated by internal magnetic stresses. The jet MHD collimation process appears to be the same at all phases, with all fast material confined within a beam diameter of about 15−20 AU over a distance ≃50 AU.

We further note that the HH212 Class 0 microjet follows interesting scalings compared with Class II microjets concerning its energetics and kinematics. (i) The mass ejection to accretion rate in HH212 estimated by Lee et al. (2007) from CO emission farther out along the jet is 15% (scaling with $V_{jet}$/100 km s$^{-1}$). This is similar to the ratio of 10% found for spatially resolved Class II jets (e.g. Woitas et al. 2002). (ii) The HH212 knot speed of 100−150 km s$^{-1}$ is typically half that in T Tauri jets (e.g. Dougados et al. 2000), for a four times lower stellar mass of 0.15 $M_\odot$ (Lee et al. 2006). Hence the jet speed appears reduced in the same proportion as the escape speed from the central object. Such scalings would be consistent with the jet acceleration mechanism and launching zone also possibly being the same at all phases. However, similar data in a larger sample of Class 0 jets would be needed to confirm this conjecture.

## 3. SiO abundance in the HH 212 microjet

### 3.1. SiO line ratios and brightness temperatures

In order to constrain the physical conditions associated with the SiO emission in the inner jet, we compared the $J = 2-1$ and 5−4 line intensities from Paper I. For proper comparison, the SiO(5−4) map, originally obtained with a 0.″78×0.″34 resolution, was reconstructed at the lower resolution of the SiO(2−1) map (1.″89 × 0.″94). Figure 3 plots on a main beam ("MB") scale the reconstructed 5−4 line profiles at the peaks of the inner SiO knots, and the ratio $T_{MB}(5-4)/T_{MB}(2-1)$ as a function of velocity (bottom panels). It can be seen that the ratio is ≃0.75−1.1 across the blue knot profile, and ≃0.5−0.85 across the red knot profile. Relative calibration uncertainties between the 2−1 and 5−4 lines are estimated to be ≃20%. We similarly evaluate the SiO (8−7) to (5−4) intensity ratio by degrading our PdBI map to the 0.″96 × 0.″69 SMA beam of Lee et al. (2007). The resulting (5−4) spectra towards the inner SiO knots are also plotted in Fig. 3. Comparison with Fig. 10 of Lee et al. (2007) yields an (8−7)/(5−4) ratio in the range 0.7−1 at all velocities. The relative calibration uncertainty could reach 30%.

A third constraint is provided by the peak main beam temperatures $T_{MB}(5-4) \simeq 25$ K in both knots in our original PdBI beam (top curve in Fig. 3). As the jet is broadened by a factor ≃2 by beam convolution across the jet (cf. Sect. 2), the intrinsic line temperature $T_R(5-4)$ is at least $25 \times 2 = 50$ K. Including beam dilution along the jet axis with 0.″78 *HPBW*, the intrinsic line brightness could reach 200 K if the knot is roughly circular.

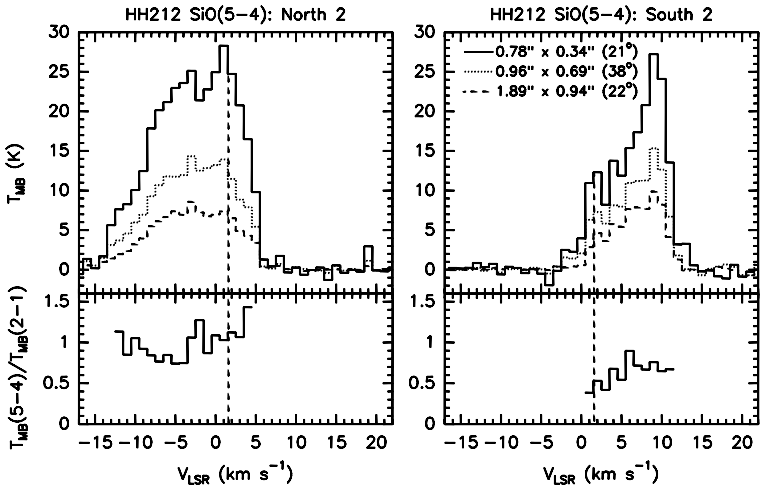


**Fig. 3.** *Top panels*: line profiles in SiO $J$ = 5−4 towards the inner SiO knots at various resolutions: the original PdBI beam (solid histogram), the SMA $J$ = 8−7 beam (dotted histogram), and the PdBI SiO $J$ = 2−1 beam (dashed histogram). Beam PAs are listed between parentheses. Note the dramatic decrease in brightness temperature with increasing beam dilution. The vertical dashed line marks the ambient LSR velocity (+1.6 km s$^{-1}$; Wiseman et al. 2001). Bottom panels: Line temperature ratio $T_{\rm MB}(5{-}4)/T_{\rm MB}(2{-}1)$ at the resolution of the PdBI SiO $J$ = 2−1 map, as a function of velocity.

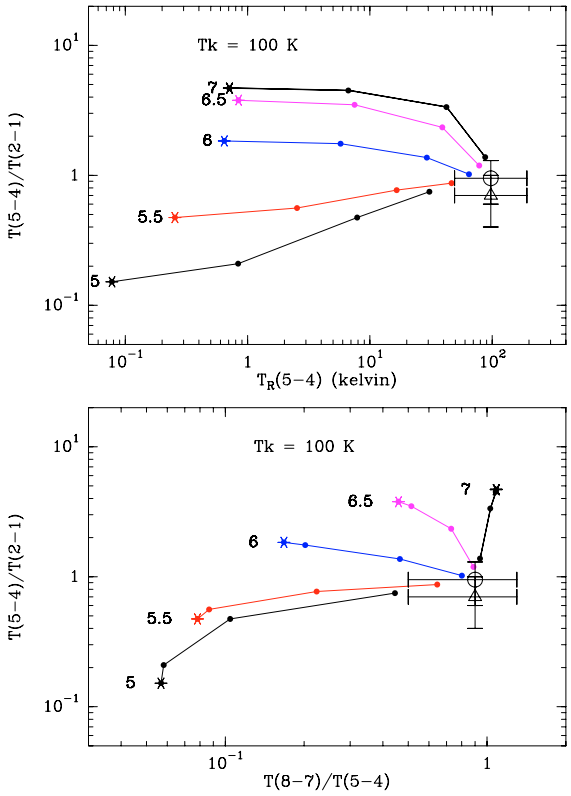


**Fig. 4.** *Top*: SiO line temperature ratio $T(5{-}4)/T(2{-}1)$ versus intrinsic line temperature $T_{\rm R}(5{-}4)$ for LVG slab models at $T_{\rm k}$ = 100 K. Each curve corresponds to the labelled $\log(n(\rm H_2))$, with dots marking values of $N_{\rm SiO}/\Delta V$ increasing (*left to right*) from $10^{12}$ to $10^{15}$ cm$^{-2}$ (km s$^{-1}$)$^{-1}$ by factors of 10. Symbols with error bars illustrate the range in line ratio in the inner SiO knots of HH212 (including calibration uncertainties) and the range in $T_{\rm R}(5{-}4)$ after correction for beam dilution. *Bottom*: same as above for the $T(5{-}4)/T(2{-}1)$ ratio versus $T(8{-}7)/T(5{-}4)$.

### 3.2. LVG modelling: evidence for optically thick SiO

The line ratios and (5−4) intrinsic brightness are compared with the result of a large velocity gradient (LVG) code, which considers the first 20 levels of SiO and the rate coefficients for collisions with $\rm H_2$ reported by Turner et al. (1992) up to $T_{\rm k}$ = 300 K. We explored $\rm H_2$ densities from $10^5$ to $10^7$ cm$^{-3}$ (see Sect. 3.3) and an LVG optical depth parameter $n(\rm SiO)/(dV/dz) = N_{\rm SiO}/\Delta V$ ranging from $10^{12}$ to $10^{17}$ cm$^{-2}$ (km s$^{-1}$)$^{-1}$, i.e. from the fully optically thin to optically thick regime. Our typical model results are illustrated graphically for $T_{\rm k}$ = 100 K in Fig. 4, and compared with observed values in HH212.

We find that the usual approach of assuming optically thin emission to derive $n(\rm H_2)$ and $T_{\rm k}$ from line ratios (e.g. Gibb et al. 2004; Nisini et al. 2007) would give inaccurate results in our case: As shown in Fig. 4 (bottom panel), no optically thin model (starred symbols in the curves) can *simultaneously* reproduce the observed values of both SiO(8−7)/(5−4) and SiO(5−4)/(2−1). Values $\simeq$ 1 for both ratios are only achieved when approaching the optically thick LTE regime ($T_{\rm R} \simeq T_{\rm k}$), which is the point of convergence of all density curves at sufficiently high opacity. We infer that $N_{\rm SiO}/\Delta V$ must be greater than $\simeq 10^{15}$ cm$^{-2}$ (km s$^{-1}$)$^{-1}$, while $n(\rm H_2)$ is not well-constrained. The high (5−4) intrinsic brightness of 50 K−200 K also independently argues for a large optical depth parameter (Fig. 4, top). It also indicates that $T_{\rm k}$ lies in the range 50−500 K, or else the predicted $T_{\rm R}(5{-}4)$ close to LTE would be too low/high.

We note that substantial SiO optical depth could be rather common in the innermost part of Class 0 jets, if they are as narrow as in HH212. In the L1448 jet, for example, a column density $\sim 10^{14}$ cm$^{-2}$ has been derived from single-dish measurements of the 5−4 transition assuming a jet width of 2″ (Nisini et al. 2007). A narrower width of ∼0.2″ would result in a column density higher by an order of magnitude, implying, as in HH212, a line optical depth larger than unity. Hence the low $T_{\rm MB}(5{-}4) \simeq$ 0.1−1 K in single-dish observations could result mainly from severe beam dilution of the SiO emission, as argued previously by Gibb et al. (2004) and illustrated in Fig. 3. The SiO abundances would then be substantially larger than previously reported.

### 3.3. SiO abundance and $H_2$ density

Noting that $N_{\rm SiO}/\Delta V = n(\rm SiO)/(dV/dz)$, the SiO abundance with respect to $\rm H_2$ may be written:

$$X(\rm SiO) \;=\; 4\times10^{-7}\left(\frac{N_{\rm SiO}/\Delta V}{10^{15}\ \rm cm^{-2}\,km^{-1}\,s}\right)\left(\frac{10^6}{n(\rm H_2)}\right) \times\left(\frac{dV/dz}{4\times10^{-11}\ \rm s^{-1}}\right). \quad (1)$$

The adopted line-of-sight velocity gradient $dV/dz$ is typical of cooled regions with $T_{\rm k} \leq$ 100 K at the rear of planar C-shocks and is probably a lower limit. A steeper gradient $dV/dz$ is given by the ratio of the FWZI of the SiO line profile ($\simeq$10 km s$^{-1}$) to the knot width (0.″2 = 100 AU), which would increase $X$(SiO) by a factor 16 from the above formula.

The main uncertainty in X(SiO) stems from the unknown $H_2$ density in the SiO knots. A reasonable range may be inferred from the presence of shock-excited $H_2O$ masers at 0.1″ from the source. Magnetic field strengths and line ratios in $H_2O$ masers around YSOs typically require preshock H nuclei densities $n_H \simeq 10^7$–$10^8$ cm$^{-3}$(Kaufman & Neufeld 1996). Assuming that density roughly drops with distance as $1/r^2$ (cf. the DG Tau jet; Lavalley-Fouquet et al. 2000), one infers a preshock density $\simeq 10^5$–$10^6$ cm$^{-3}$ at the SiO knots. Shock compression could increase these values by a about an order or magnitude (e.g. Kaufman & Neufeld 1996), so that the density is in the range $\simeq 10^5$–$10^7$ cm$^{-3}$. The resulting *minimum* SiO abundance for optically thick emission is $X(\mathrm{SiO}) \geq (4 \times 10^{-8}$–$4 \times 10^{-6}) \times$ (1–16), with the higher value corresponding to the lower density, and the additional factor 1–16 arising from the uncertainty in velocity gradient. Assuming a solar abundance of $(\mathrm{Si/H})_\odot \simeq 3.5 \times 10^{-5}$ (Grevesse & Sauval 1998), between 0.05% and 90% of the elemental silicon is in the form of SiO.

### 3.4. Origin of the SiO component

Our PdBI observations of the HH212 microjet set stronger constraints than previously on the origin of the SiO in protostellar outflows, because of the shorter timescales involved and the unusually high collimation and SiO column densities indicated by our data.

Given the proper motions of 60–150 km s$^{-1}$ for $H_2O$ masers and $H_2$ knots (Claussen et al. 1998; McCaughrean et al. 2002), the dynamical time of inner SiO peaks at 500 AU is only 25 yr. SiO should thus be incorporated very rapidly in the flow. The formation of SiO in outflows is usually attributed to sputtering of Si atoms from charged grains in a magnetized C-shock with ion-neutral drift speeds $\geq$25 km s$^{-1}$ (Schilke et al. 1997). Updated C-shock models with improved sputtering yields, SiO formation rates, and molecular cooling (Gusdorf et al., in preparation) show that the required conditions for optically thick emission are reached for shock speeds 35–45 km s$^{-1}$ and preshock densities of $10^5$–$10^6$ cm$^{-3}$ but only at the rear of the shock where velocity gradients are small, i.e. after 400–150 yrs. As this exceeds the knot dynamical time, non-steady truncated C-shocks need to be considered to model SiO-emitting shocks on such small scales.

Another long-standing issue is whether SiO molecules originate from shocked ambient material or trace the primary jet itself. The SiO microjet diameter of 100 AU is comparable to the centrifugal disk diameter of 120 AU indicated by our 1mm continuum size (Paper I) and by envelope kinematics (Lee et al. 2006). Hence we would expect little infalling molecular material left on-axis to refill the jet path between successive ejection episodes, unless this material is very warm. This would appear to favor an origin of the SiO in the jet itself. The option is appealing, as the higher densities of Class 0 jets, and the accompanying low temperature and ionization, are indeed conducive to molecular formation. In an early study of chemistry in protostellar winds, Glassgold et al. (1991) found that Si atoms are quickly converted into SiO at high mass-loss rates $\dot{M}_{\rm jet} > 10^{-6} M_\odot$ yr$^{-1}$. For a dust-free wind, the predicted SiO abundances are $\simeq$50–100% of the total elemental silicon. However, the recent finding of a substantial depletion of Fe and Ca at the base of several Class I jets (Podio et al. 2006) indicates that jets are not dust-free and that grains are only partly eroded along the flow. In the HH34 jet, 13% of Fe has been returned to the gas at distances $\geq$1500 AU. The same process at work in Class 0 jets would release Si atoms in a sufficient amount to produce optically thick SiO emission if $\dot{M}_{\rm jet} \geq 10^{-6}\ M_\odot$ yr$^{-1}$. In the inner SiO knots of HH212, this mass-flux is achieved for $n(\mathrm{H_2}) \geq 10^6$ cm$^{-3}$ (with $V_{\rm jet} = 100$ km s$^{-1}$ and a jet radius of 50 AU), thus only 0.5%–9% of Si would be needed, if all is converted into SiO (see Eq. (1)).

## 4. Conclusions

Our finding that jet collimation in the HH212 Class 0 source is similar to that in T Tauri stars favors a collimation mechanism independent of the presence of a dense envelope, i.e. most probably internal MHD stresses. The ejection/accretion ratio and the jet speed/escape speed ratio also appear to be similar to those in Class II, possibly suggesting the same acceleration mechanism as well. The main difference between Class 0 jets and their more evolved analogs would then be their differing chemical composition, with abundant molecules at the Class 0 stage, a mixed atomic-molecular composition at the Class I stage (Davis et al. 2001, 2003), and a purely atomic flow at the Class II stage.

We also find that SiO is optically thick, so that its abundance is larger than previously estimated. The extremely narrow width of the SiO jet revealed by PdBI further argues that this species is not formed in swept-up material, but more likely within the jet itself. We thus propose that the higher SiO content of Class 0 jets could mainly reflect an increase in jet density (hence, a higher efficiency of molecular formation), linked to the increased mass-accretion rate at earlier stages.

*Acknowledgements.* We are grateful to R. Cesaroni, J. Ferreira, and an anonymous referee for helpful comments. This work is supported in part by the European Community's Marie Curie Research Training Network JETSET under contract MRTN-CT-2004-005592. It benefited from research funding by the European Community's sixth Framework Programme under RadioNet R113CT 2003 5058187. A. Gusdorf acknowledges support through the European Community's Human Potential Programme under contract MRTN-CT-2004-512302, Molecular Universe.

## References

Chandler, C. J., & Richer, J. S. 2001, ApJ, 555, 139
Claussen, M. J., Marvel, K. B., Wootten, A., & Wilking, B. A. 1998, ApJ, 507, L79
Codella, C., Cabrit, S., Gueth, F., et al. 2007, A&A, 462, L53 (Paper I)
Davis, C. J., Ray, T. P., Desroches, L., & Aspin, C. 2001, MNRAS, 326, 524
Davis, C. J., Whelan, E., Ray, T. P., & Chrysostomou, A. 2003, A&A, 397, 693
Dougados, C., Cabrit, S., Lavalley-Fouquet, C., & Ménard, F. 2000, A&A, 357, L61
Delamarter, Frank, & Hartmann 2000, ApJ, 530, 923
Gibb, A. G., Richer, J. S., Chandler, C. J., & Davis, C. J. 2004, ApJ, 603, 198
Glassgold, A. E., Mamon, G. A., & Huggins, P. J. 1991, ApJ, 373, 254
Grevesse, N., & Sauval, A. J. 1998, Space Sci. Rev., 85, 161
Gueth, F., et al. 2007, in preparation
Guilloteau, S., Bachiller, R., Fuente, A., & Lucas, R. 1992, A&A, 265, L49
Hirano, N., Liu, S.-Y., Shang, H., et al. 2006, ApJ, 636, L141
Kaufman, M. J., & Neufeld, D. A. 1996, ApJ, 456, 250
Lavalley-Fouquet, C., Cabrit, S., & Dougados, C. 2000, A&A, 356, L41
Lee, C.-F., Ho, P. T. P., Beuther, H., et al. 2006, ApJ, 639, 292
Lee, C.-F., Ho, P. T. P., Beuther, H., et al. 2007, ApJ, in press
McCaughrean, M., Zinnecker, H., Andersen, M., Meeus, G., & Lodieu, N. 2002, Msngr, 109, 28
Nisini, B., Codella, C., Giannini, T., et al. 2007, A&A, 462, 163
Palau, A., Ho, P. T. P., Zhang, Q., Estalella, R., et al. 2006, ApJ, 636, L137
Podio, L., Bacciotti, F., Nisini, B., et al. 2006, A&A, 456, 189
Schilke, P., Walmsley, C. M., Pineau des Forêts, G., & Flower, D. R. 1997, A&A, 321, 293
Turner, B. E., Chan, K. W., Green, S., & Lubowich, D. A. 1992, ApJ, 399, 114
Woitas, J., Ray, T. P., Bacciotti, F., Davis, C. J., & Eislöffel, J. 2002, ApJ, 580, 336
Wiseman, J., Wootten, A., Zinnecker, H., & McCaughrean, M. 2001, ApJ, 550, L87